Nuclear Instruments and Methods in Physics Research B 269 (2011) 1444–1449

Contents lists available at ScienceDirect

Nuclear Instruments and Methods in Physics Research B

journal homepage: www.elsevier.com/locate/nimb

Monte Carlo simulation of spectrum changes in a photon beam due to a brass compensator

E.R. Custidiano [a,*], M.R. Valenzuela [a], J.L. Dumont [b], J. McDonnell [c], L Rene [d], J.M. Rodríguez Aguirre [a]

[a] Department of Physics, FaCENA, UNNE, Av., Libertad 5470, C.P.3400, Corrientes, Argentina
[b] Elekta CMS Software, St.Louis, MO, USA
[c] Cumbres Institute, Riobamba 1745, C.P.2000, Rosario, Santa Fe, Argentina
[d] Radiotherapy Center, Crespo 953, C.P.2000, Rosario, Santa Fe, Argentina

ARTICLE INFO

Article history:
Received 3 March 2011
Received in revised form 22 March 2011
Available online 26 March 2011

Keywords:
Radiotherapy
IMRT
Compensators
Monte Carlo
Spectra

ABSTRACT

Monte Carlo simulations were used to study the changes in the incident spectrum when a poly-energetic photon beam passes through a static brass compensator. The simulated photon beam spectrum was evaluated by comparing it against the incident spectra. We also discriminated the changes in the transmitted spectrum produced by each of the microscopic processes. (i.e. Rayleigh scattering, photoelectric effect, Compton scattering, and pair production). The results show that the relevant process in the energy range considered is the Compton Effect, as expected for composite materials of intermediate atomic number and energy range considered.

1. Introduction

Solid compensators are used as beam modulators to produce non-uniform photon fluence for Intensity-Modulated Radiotherapy (IMRT) [1–4]. Between the parameters of dosimetric interest are the mass attenuation coefficient, effective atomic number, electron density and energy spectra; these characterize photon interactions with composite materials.

An important process involved in the attenuation of a photon beam passing through a static compensator is the change in the energy distribution of photons, i.e. the change in beam energy spectrum, the so-called beam hardening. Therefore the determination of such changes is necessary any time a calculation algorithm is used that starts with an incident spectrum at the patient surface level and could, in principle, be used to improve the dosimetric accuracy of such algorithm. It is important to note that several experimental methods and simulations have been reported in the literature for its determination [5–7]. Of these simplest, by far, is the spectral reconstruction from attenuation data or transmission [8–10]. An alternative way of approaching the problem of knowing the energy spectrum of a photon beam incident on the surface of a material medium, having previously passed through a static compensator is Monte Carlo (MC) simulations; for which it is essential to know the incident spectrum. Direct measurements of the high-energy photon beam spectra emitted in short pulses by Linacs is very difficult mainly due to the high dose rate of the beam, which precludes the utilization of multichannel analyzers. In general, the incident spectra used are those published [11–13], and although those can contain some inaccuracies or be incomplete in nature, they are sufficient to characterize the spectrum changes, by comparison of the input vs. the transmitted spectra after passing through the compensator.

The purpose of this study is to investigate, by MC simulations [6], the changes experienced by a photon beam spectra when it passes through a compensator, by analyzing the primary beam attenuation and the role played by each fundamental microscopic processes. The subsequent dosimetric implications were also analyzed [14,15].

1.1. Methodology

When we analyze all the steps involved in treatment planning and subsequent implementation using the IMRT method we note that one of them is the interaction of radiation with the compensator in which, unlike the interaction with the target volume in which important is the effect of radiation on the biological system, is essential to determine and understand the effect of the

* Corresponding author. Tel.: +54 03783 457950 117.
E-mail addresses: ernesto7661@gmail.com (E.R. Custidiano), meraqval@gmail.com (M.R. Valenzuela), Joseluis.Dumont@elekta.com (J.L. Dumont), josemc@express.com.ar (J. McDonnell), luismrene@gmail.com (L Rene), juakcho@gmail.com (J.M. Rodríguez Aguirre).

0168-583X/$ - see front matter © 2011 Elsevier B.V. All rights reserved.
doi:10.1016/j.nimb.2011.03.020

compensator on the parameters that characterize the photon beam. An important effect is the energy fluence modulation.

Spectra calculated with the MC method can be used as reference data for the calculation of all other approaches. This method actually requires specific knowledge of the components of the accelerator head, which limits their widespread use. But a way to avoid this difficulty is to use a spectrum obtained by simulation as incident. This is the method that is used in this work [11]. This latter is especially valid if we consider that in most cases it is hard to obtain the precise characteristics of the components of the accelerator head. In MC simulations when the beam passes through compensator, components are separated into primary and secondary components, and the separation of absorbed dose into primary dose contribution, due to the electrons liberated by photons that interact with the medium for the first time, and scattered dose, due to electrons liberated by photons that have interacted with the medium more than once [16].

1.2. Experiments

The experimental setup consisted of homogeneous brass sheets covering the whole radiation field. The sheets were placed on a polymethylmethacrylate (PMMA) shadow tray at 65 cm from the photon source, and transmission measurements with a diode array were performed using the 6 MV energy beam generated in an Elekta Precise Linac. A square hole was cut in the tray to avoid PMMA interaction. The experimental values were obtained using a PROFILER2 diode array (Sunnnuclear Corp.) running the software version 1.3.0.0, located over the treatment table perpendicular to the vertical beam axis. The field size was adjusted to a symmetric $3 \times 3\ cm^2$ and $10 \times 10\ cm^2$ at 100 cm from the source. A $20 \times 20 \times 20\ cm^3$ PMMA small water phantom was located over the PROFILER2 to provide an adjustable water depth. This depth was fixed in 10 cm water equivalent, obtained with 1 cm of virtual water included in the PROFILER2, 4 mm of the PMMA water phantom bottom thickness, and 8.55 cm of water. The Source Surface Distance (SSD) was adjusted to 100 cm. The profiles values obtained irradiating 100 MU (denote the monitor chamber reading for a specified amount of radiation from a radiotherapy treatment machine, i.e. a clinical accelerator [17]) were recorded for the open field and different brass sheets thickness, ranging from 1 to 5 cm. The Percent Depth Dose (PDD) in water for the symmetric $3 \times 3\ cm^2$ and $10 \times 10\ cm^2$ open fields in water was obtained using a Scanditronix RFA200 automatic water phantom at SSD = 100 cm.

1.3. Simulations

MC Simulations were performed to reproduce the experimental design described above and the simulated values were compared with the experimental data.

In this work we used the PENELOPE [18] MC code to simulate a 6 MV Elekta Linac photon beam.

PENELOPE is a general purpose package for radiation transport simulation in an arbitrary material defined by its composition. The phase space files contain the angle, energy and charge of the particles in the mixed photon-electron beam and it was used as an incident to obtain the beam energy spectra after crossing the compensator.

1.4. Principio del formulario

The geometry used consisted of a 6 MV point source located 100 cm of water phantom, between the source and the phantom was filled with moist air. The brass sheet was placed at 65 cm from the source, covering the entire field of radiation, using 5 cm of brass for the field of $10 \times 10\ cm^2$and 4 cm of brass for the field of $3 \times 3\ cm^2$. The incident spectrum used was obtained from [11,19]. The water phantom used is infinity sideways; with 30 cm of depth. The used voxel size was $0.5 \times 0.5 \times 0.3$ cm in x, y, z respectively. A total of 1.0×10^8 histories were simulated for $3 \times 3\ cm^2$ and $10 \times 10\ cm^2$ fields, using the modular quadric PENGEOM package [18](Chapter 5).

The calculation algorithm is controlled by four tracking parameters, C_1, C_2, W_{cc} and W_{cr}. Where C_1 and C_2 refer to elastic collisions, C_1 provides a measure of the average angular deflection due to elastic hard collisions; C_2 determines the maximum fractional energy loss between hard elastic events. The cutoff energies W_{cc} and W_{cr} have an important effect on simulated energy distributions [19]. In this paper we choose a set of tracking parameters of the PENELOPE code, which better fit the experimental curves of the PDD, in water at a $10 \times 10\ cm^2$ field, of a 6 MV photons beam generated by an Elekta Precise Linac, passing through a brass compensator of 5 cm thick. The set of tracking parameters used were: $E_{abs1} = 1.0 \times 10^4$ eV; $E_{abs2} = 1.0 \times 10^4$ eV; $E_{abs3} = 1.0 \times 10^4$ eV; C_1 and $C_2 = 0.07$; and $W_{cc} = 1.0 \times 10^5$ eV and $W_{cr} = 1.0 \times 10^4$ eV.

The materials [20] used in the simulations are outlined in Table 1.

The incident spectrum was obtained from published data [11], and the transmitted spectrum after the compensator was obtained by storing in a phase space file the parameters of the particles emerging on the distal side of the compensator. The primary interactions were separated by each of the microscopic processes. (i.e. Rayleigh scattering, photoelectric effect, Compton scattering, and pair production).

The simulated percent depth dose in the central axis and the dose profile at 10 cm, originated by the incident photon beam in the water phantom after crossing the compensator, were compared with measured values to assess the practical effect of the beam hardening in a known dose distribution.

2. Results and discussion

MC simulations of photon beam generated by a 6 MV Elekta linacs with a $3 \times 3\ cm^2$ and $10 \times 10\ cm^2$ fields, impinging on the surface of a water phantom located at 100 cm from the source, were performed.

For partial validation we calculated with statistical uncertainty of 0.6% and less than 2% experimental uncertainty, the percentage depth dose, Fig. 1a; the dose profile at 10 cm depth, with statistical uncertainty of 0.8% and less than 1.4% experimental uncertainty, Fig. 1b.

To validate the brass material we calculated for fields of $3 \times 3\ cm^2$ and $10 \times 10\ cm^2$, the ratio between the depth dose on the central axis for open and blocked fields, with different thicknesses of brass; with statistical uncertainty of 1.2% and 1% and less than 1% and 1.5% experimental uncertainty, for the field of $3 \times 3\ cm^2$ and $10 \times 10\ cm^2$ respectively, Figs. 2a and 2b.

Assuming that the MC calculations of the spectral changes are accurate, the agreement of the data calculated and measured depth dose and dose profiles implies the truth of the calculated data. The reverse is not necessarily true. [21,22]

The MC simulation results of a 6 MV photons beam, with a standard spectrum as incident [11], incident on a brass compensator shows the significant changes in the transmitted spectrum. Figs. 3a and 3b shows the transmitted energy spectrum of a 6 MV photon beam from of a compensator of 4 and 5 cm thickness compared with the incident spectra, for the field of $3 \times 3\ cm^2$ and $10 \times 10\ cm^2$ respectively. We can observe how the transmitted energy spectra decreases in the entire energy range considered and shifts to the high energy region due to preferential attenuation of lower energy photons. This is the so-called hardening processes

Table 1
Materials used in the simulations. The compositions are expressed in mass percentage.

Material	Density (g/cm^3)	Composition (%)						
		H	O	C	N	Ar	Cu	Zn
Humid Air	1.263×10^{-3}	4.0	19.42	0.015	75.635	0.485	–	–
Liquid water	1.0	2.0	1.0	–	–	–	–	–
Brass	8.9	–	–	–	–	–	66.0	34.0

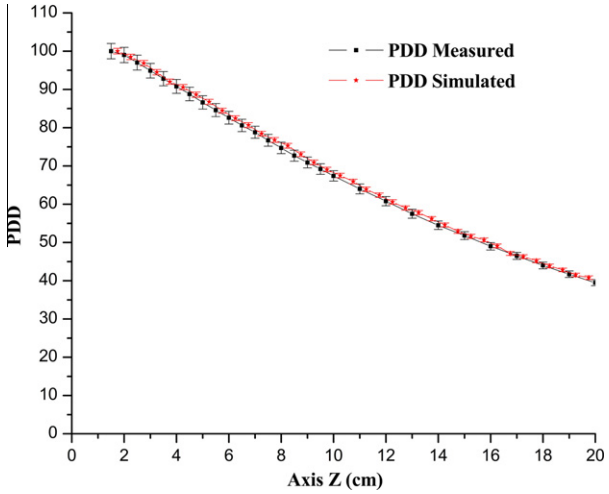

Fig. 1a. Comparison of percent depth simulated and measured. Open field 10×10 cm^2 Elekta Precise-SL-18, 6 MV photon. DFS = 100 cm.

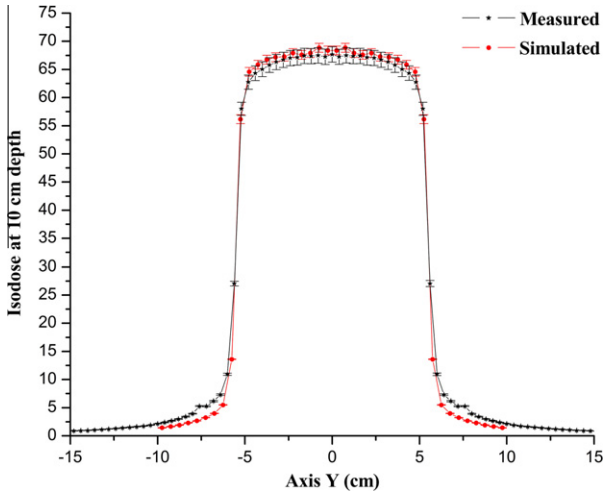

Fig. 1b. Comparison of the dose profile at dose 10 cm depth simulated and measured. Open field 10×10 cm^2 Elekta Precise-SL-18, 6 MV photon. DFS = 100 cm.

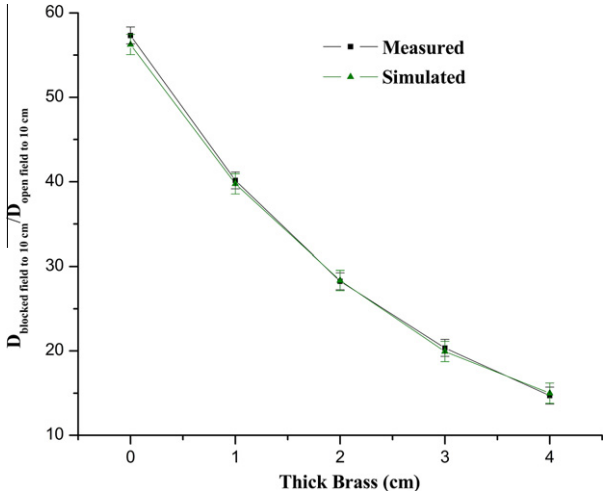

Fig. 2a. Comparison of ratio of d10 blocked vs open as a function of block thickness. For blocked and open 3×3 cm^2 fields simulated and measured. Elekta Precise-SL-18, 6 MV photon. DFS = 100 cm.

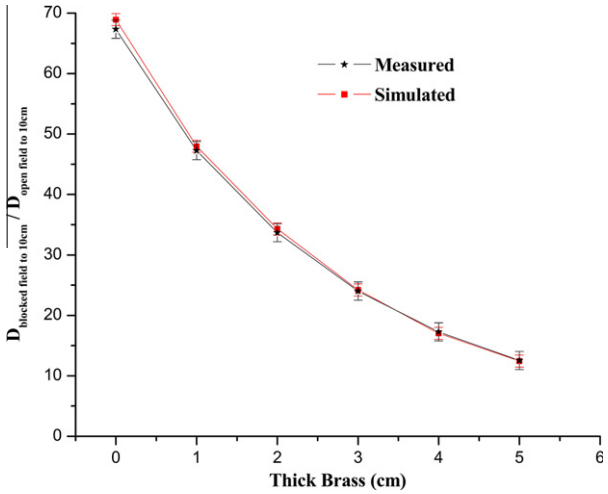

Fig. 2b. Comparison of ratio of d10 blocked vs open as a function of block thickness. For blocked and open 10×10 cm^2 fields simulated and measured. Elekta Precise-SL-18, 6 MV photon. DFS = 100 cm.

by which the low energy photons preferentially interact with the medium.

Fig. 4a shows the comparison of the PDD simulation of a 10×10 cm^2 field, with the incident and transmitted spectra, each normalized to itself, and we can observe the change in the penetration of the beam before and after compensating for the effect of beam hardening. The net effect is approximately 1.3% of the dose at 5 cm depth and 2.2% at 10 cm depth, while at 15 cm depth the difference is about 3.4%. With statistical uncertainty 0.8% for the open field and 2% for the blocked field. Fig. 4b shows the comparison of the measured PDD for a 10×10 cm^2 field, with the incident and transmitted spectra, each normalized to itself, and we can observe the change in the penetration of the beam before and after the compensator by the beam hardening effect. The net effect is approximately 1.3% of the dose at 5 cm depth and 2.4% at 10 cm depth, while at 15 cm depth; the difference is about 4.0%. With experimental uncertainty of 0.3% for the open field and 3% for the blocked field.

Fig. 5a shows the comparison of the PDD simulation of a 3×3 cm^2 field, with the incident and transmitted spectra, each normalized to itself, and we can observe the change in the penetration of the beam before and after compensating for the effect of

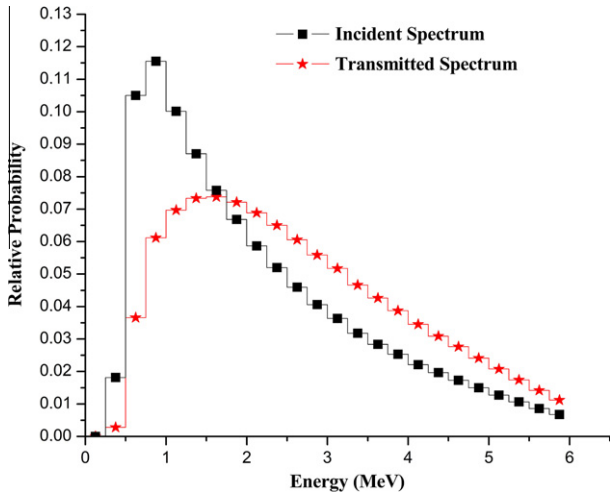

Fig. 3a. Comparison between incident and transmitted spectrum resulting. Each spectrum is normalized to itself. Field 3×3 cm^2.

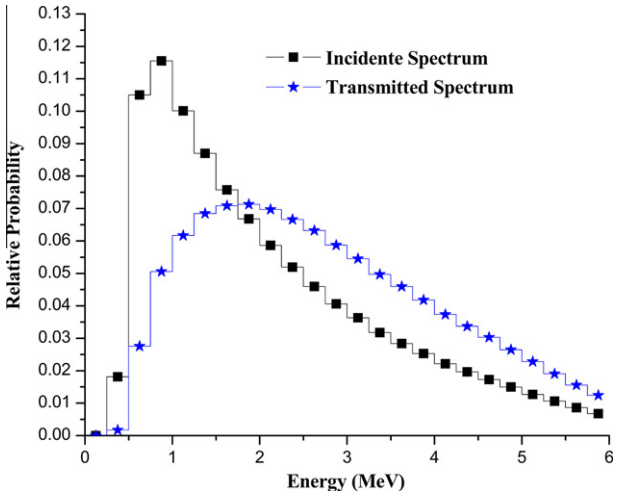

Fig. 3b. Comparison between incident and transmitted spectrum resulting. Each spectrum is normalized to itself. Field 10×10 cm^2.

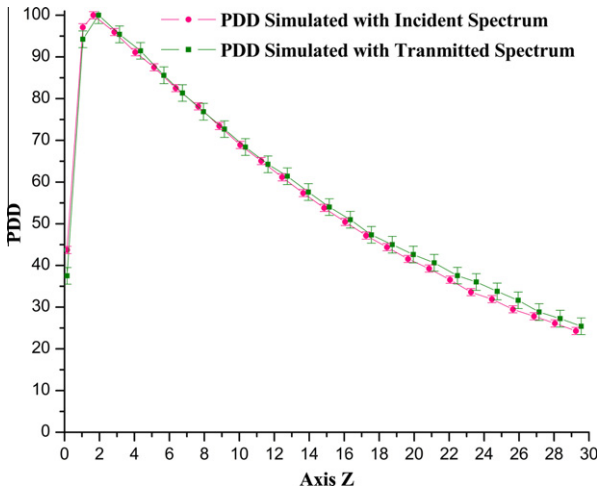

Fig. 4a. Comparison between PDD simulated, with incident and transmitted spectrum. Each PDD is normalized to itself. Field 10×10 cm^2.

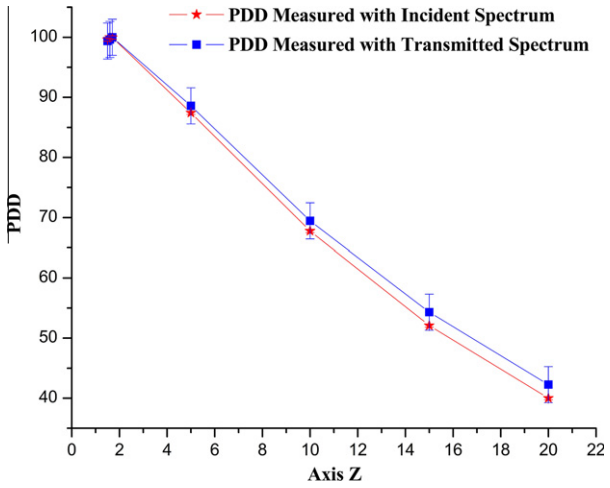

Fig. 4b. Comparison between PDD measured, with incident and transmitted spectrum. Each PDD is normalized to itself. Field 10×10 cm^2.

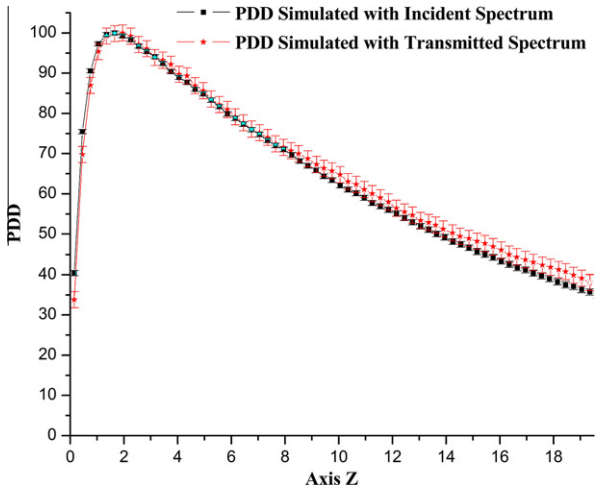

Fig. 5a. Comparison between PDD simulated incident and transmitted spectrum. Each PDD is normalized to itself. Field 3×3 cm^2.

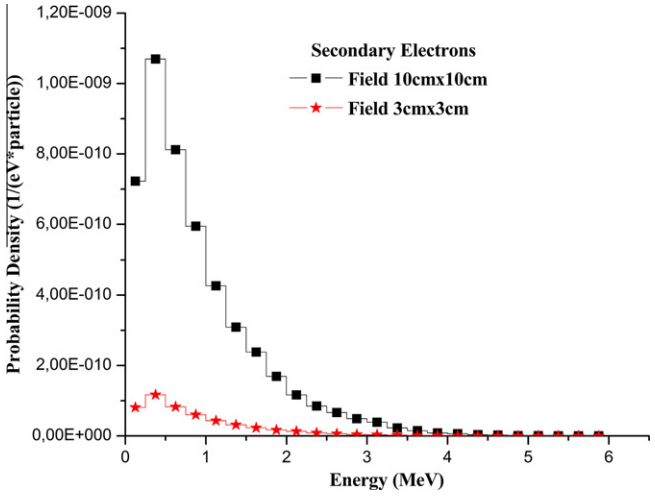

Fig. 5b. Comparison between 3×3 and 10×10 cm^2 fields. Secondary electrons generated in brass that reach the phantom surface.

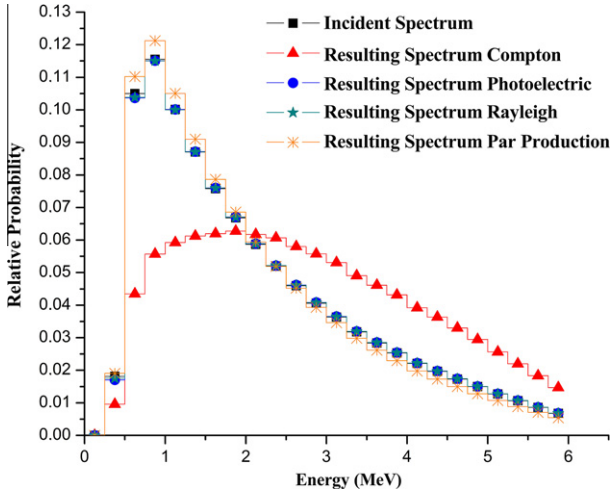

Fig. 6a. Comparison between the incident spectrum and the spectrum resulting from subtracting the spectrum incident each microscopic processes occurring in the compensator. Field 3×3 cm^2.

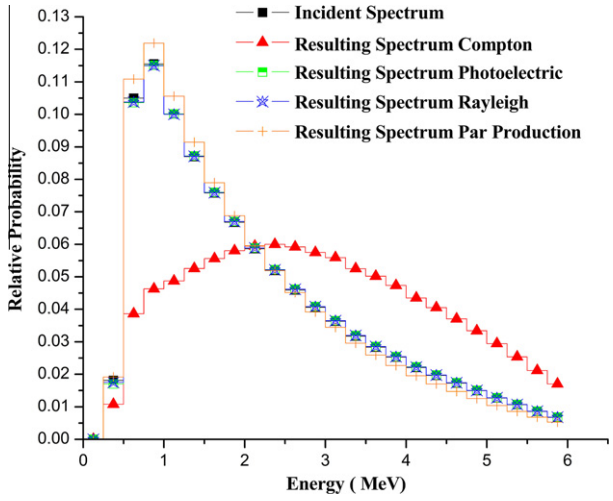

Fig. 6b. Comparison between the incident spectrum and the spectrum resulting from subtracting the spectrum incident each microscopic processes occurring in the compensator. Field 10×10 cm^2.

beam hardening. The net effect is approximately 0.6% of the dose at 5 cm depth and 2.4% at 10 cm depth, while at 15 cm depth the difference is 5.0%. With statistical uncertainty 0.7% for the open and 2% for the blocked field.

Fig. 5b. shows the comparison between 3×3 cm^2 and 10×10 cm^2 fields, of secondary electrons generated in brass that reach the phantom surface, and we observe, as expected, that for a 10×10 cm^2 field the number of secondary electrons generated in the brass, which reach the surface of the water phantom is higher.

For the purpose of elucidating the events responsible for the changes in the transmitted spectrum, partial contributions were scored for each of the microscopic processes that occur in the energy range considered and the corresponding Z_{eff}, (i.e. Compton, photoelectric, pair production and Rayleigh processes), Figs. 6a and 6b.

As expected they shows that the most important change is due to the Compton Effect, whereas the changes caused by the photoelectric effect, pair production and Rayleigh are negligible. The results agree well with those reported in the literature for materials

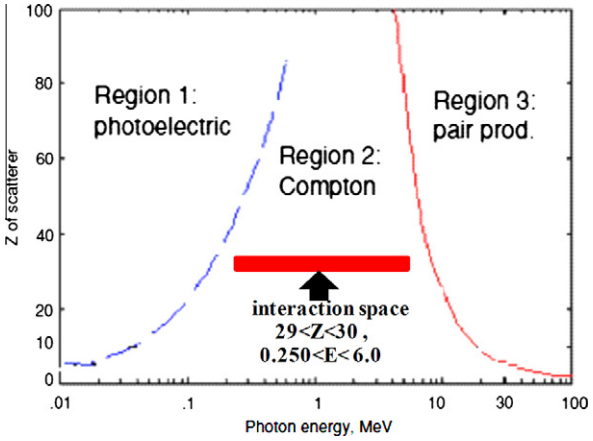

Fig. 7. Relative importance of the microscopic events occurring in the photon beam – matter interaction. The lines show the energy and Z values for which two neighboring microscopic events are equal.

of intermediate atomic number, in which the attenuation coefficient varies slowly with energy and allows the reconstruction of the spectrum by analyzing the scattered radiation in an experimental set-up where the Compton interaction predominates [21].

The results are consistent with those reported in literature for brass, where the Compton effect appears to be the relevant process for incident photon energies ranging between 0.2 keV and 5 MV; with the effective atomic number constant in that energy range [21,22] Fig. 7, shows the relative importance of microscopic events that occur in the interaction of photons beam and matter and we can see too that the range of the photon beam energy spectra and the corresponding brass Z_{effec} are in the entire Compton domain [23].

3. Conclusion

This work emphasizes the importance of beam hardening in the process of beam modification by metal modifiers like compensators and physical wedges. In particular, it provides a quantitative estimation of the increase in absorbed dose as a consequence of increased effective energy.

We conclude that a spectrum modification based solely in Compton interactions is enough to account for the majority of the effects observed in the beam hardening process, with pair production only marginally affecting the 6 MV, which means it can be ignored as well. This opens the door to a simplified beam hardening based in Compton interactions only, with the associated speed up of calculations.

We also provide the modified spectrum coming out of the 5 cm thick brass compensator, which can be of importance for MC simulations based in an incident spectrum in the patient surface, as opposed to modifying the spectrum as part of the beam attenuation process. A number of commercial implementations of MC calculations do not currently support transport trough high Z beam modifiers and the associated spectrum modification, hence the importance of obtaining a modified spectrum by other means.

Acknowledgments

We thank, specially, to OECD Nuclear Energy Agency for providing us with the PENELOPE 2006 Code needed for MC simulations. This work was partially supported by PI/07/2007 Secretaría Gral. de Ciencia y Téenica - UNNE, SPU - Programa Voluntariado 2007 and FaCENA-UNNE. Two of the authors (MRV and JMRA) wish to thanks the CONICET for the financial support.

References

[1] J.A. Purdy, Int. J. Radiat. Oncol. Biol. Phys. 35 (1996) 845–846.
[2] T. Knoos, L. Wittgren, Phys. Med. Biol. 36 (1991) 255–267.
[3] S. Webb, Br. J. Radiol. 76 (2003) 678–689.
[4] B.E. Bjarngard, H. Shackford, Med. Phys. 21 (1994) 1069–1073.
[5] A. Piermattei, G. Arcovito, L. Azario, L. Bacci, L. Bianciardi, E. de Sapio, C. Giacco, Med. Phys. 17 (1990) 227–233.
[6] R. Mohan, C. Chui, L. Lidofsky, Med. Phys. 12 (1985) 592–597.
[7] B.A. Faddegon, C.K. Ross, D.W.O. Rogers, Med. Phys. 17 (1990) 773–785.
[8] C.R. Baker, B. Ama'ee, N.M. Spyrou, Phys. Med. Biol. 40 (1995) 529–542.
[9] C.R. Baker, K.K. Peck, Phys. Med. Biol. 42 (1997) 2041–2051.
[10] R.G. Waggener, M.M. Blough, J.A. Tery, J.A. D.Chen, N.E. Lee, S. Zhang, W. D. Med. Phys. 26 (1999) 1269–1278.
[11] D.S. Bagheri, D.W.O. Rogers, Med. Phys. 29 (2002) 391–402.
[12] R. Mohan, C. Chui, L. Lidofsky, Med. Phys. 13 (1986) 64–73.
[13] D.W. Rogers, B.A. Faddegon, G.X. Ding, C.M. Ma, J. We, T.R. Mackie, Med. Phys. 22 (1995) 503–524.
[14] S.X. Chan, T.J. Cullip, K.M. Deschesne, Med. Phys. 27 (2000) 948–959.
[15] P.C. Shragge, M.S. Patterson, Med. Phys. 8 (1981) 885–891.
[16] P. Nizin, G.X. Qian, H. Rashid, Med. Phys. 20 (1993) 1353–1360.
[17] C.M. Ma, R.A. Price Jr., J.S. Li Chen, L. Wang, E. Fourkal, L. Qin, Yang, Phys. Med. Biol. 49 (2004) 1671–1687.
[18] F. Salvat, J.M. Fernández-Varea, J. Sempau, Penelope-2006: A Code System for Monte Carlo Simulation of Electron and Photon Transport, Workshop Proceedings Barcelona, Spain, 2006.
[19] J. Baro, J. Sempau, J.M. Fernández-Varea, F. Salvat, Nucl. Inst. and Meth. Phys. Res. B 100 (1995) 31–46.
[20] T. Ivanova, G. Malatara, K. Bliznakova, D. Kardamakis, N. Pallikarakis, 11th Mediterranean Conference on Medical and Biomedical Engineering and Computing 2007, IFMBE Proceedings) vol. 16 (2007) 923–927.
[21] M. Partridge, Phys. Med. Biol. 45 (2007) N115–N131.
[22] W.T. Jalbout, N.M. Spyrou, Phys. Med. Biol. 51 (2006) 2211–2224.
[23] S.R. Manohara, S.M. Hanagodimath, K.S. Thind, L. Gerward, Nucl. Inst. and Meth. Phys. Res. B 266 (2008) 3906–3912.